

Modeling of Wax Precipitation in Crude Oils

by

Chin Kim Foh

Dissertation submitted in partial fulfilment of
the requirements for the
Bachelor of Engineering (Hons)
(Chemical Engineering)

JANUARY 2010

Universiti Teknologi PETRONAS
Bandar Seri Iskandar
31750 Tronoh
Perak Darul Ridzuan

CERTIFICATION OF APPROVAL

Modelling of Wax Precipitation in Crude Oils

by

Chin Kim Foh

A project dissertation submitted to the
Chemical Engineering Programme
Universiti Teknologi PETRONAS
in partial fulfilment of the requirement for the
BACHELOR OF ENGINEERING (Hons)
(CHEMICAL ENGINEERING)

Approved by,



(Professor Dr. **MUHGESAN**
PROF. DR. MUHABBALAH MUHSEN)
Chemical Engineering Department
Universiti Teknologi PETRONAS

UNIVERSITI TEKNOLOGI PETRONAS

TRONOH, PERAK

January 2010

CERTIFICATION OF ORIGINALITY

This is to certify that I am responsible for the work submitted in this project, that the original work is my own except as specified in the references and acknowledgements, and that the original work contained herein have not been undertaken or done by unspecified sources or persons.



CHIN KIM FOH

ABSTRACT

Production of crude oil from high temperature reservoir from subsurface to surface will reduce the oil temperature and it will lead to formation of wax. The wax precipitation is common in petroleum industry which gives challenges to the flow assurance. The major problems that caused by wax formation are reduction of production, increased pressure drop in pipeline, and high risk of getting a pipeline gauge stuck during maintenance operations. It can be very costly to solve the problems caused by wax and may lead to loses. The objective of this project is to develop an thermodynamic model to predict the Wax Appearance Temperature (WAT) by determining the suitable solubility parameters, fusion enthalpies and fusion temperatures. Recognizing the WAT may improve cost saving of crude oil production. Early prevention can be carried out to avoid wax precipitation in the operating facilities and maintain the performance and efficiency of equipments. In order to produce an accurate model in predicting wax forming temperature, the liquid-solid transition factors need to be considered. The thermodynamic model for estimation of WAT is being developed by finding the details of each parameter which will be inserted into MATLAB for calculation. The effect of carbon numbers, fusion enthalpies and solubility parameters to the model has been obtained. The results of this model have been compared with the existing model. In conclusion, the suitable parameters for the wax prediction model have been determined and a thermodynamic model has been developed to predict WAT and wax amount.

ACKNOWLEDGEMENTS

I wish to take this opportunity to express my gratitude to the individuals that have contributed to the completion of this project. First and foremost, many thanks to the university and the final year project coordinators who have coordinated and made the necessary arrangements for all the activities related to final year project.

The utmost gratitude goes to my project supervisor, Professor Dr Thanabalan Murugesan, who has been guiding and providing me with endless support. His supervision has been great in directing me through the right path towards the completion of this project.

Lastly, I would like to acknowledge all individuals that have helped me and given me guidance directly and indirectly throughout the project period. The support and kindness from the people above will always be a pleasant memory. Thank you.

TABLE OF CONTENTS

ABSTRACT	i
ACKNOWLEDGEMENTS	ii
CHAPTER 1: INTRODUCTION	1
1.1 Background of Study	1
1.2 Problem Statement	2
1.3 Objectives.....	3
1.4 Scope of Study	3
1.5 Relevancy of the Project	4
1.6 Feasibility of Project	4
CHAPTER 2: LITERATURE REVIEW	5
2.1 Physical Properties of Wax.....	5
2.2 Molecular Diffusion, Brownian Diffusion, Shear Dispersion and Gravity Settling	5
2.3 Mechanism of Paraffin Wax Crystallization.....	6
2.4 Thermodynamic Models	7
2.5 Thermodynamic Equations	10
2.5.1 Activity Coefficients	12
2.5.2 Liquid and Solid Phase Solubility Parameters	13
2.5.3 Liquid and Solid Phase Heat Capacity.....	16
2.5.4 Fusion Enthalpy.....	17
2.5.5 Solid-solid Transition.....	20
CHAPTER 3: METHODOLOGY	21
3.1 Computational Processes	22
3.2 Gantt Chart.....	24
CHAPTER 4: RESULTS AND DISCUSSION	25

4.1 Data Gathering	25
4.2 Modeling Results	28
4.2.1 Effect of Carbon Number	29
4.2.2 Effect of Fusion Enthalpy	31
4.2.3 Effect of Solubility Parameters	33
4.2.4 Effect of Solid-solid Transition.....	35
4.2.5 Comparison of Model.....	36
4.2.6 Potential Errors.....	39
CHAPTER 5: CONCLUSION AND RECOMMENDATION	40
5.1 Conclusion	40
5.2 Recommendation	41
REFERENCES.....	42
APPENDICES	44

LIST OF FIGURES

Figure 1: Cross-sectional view of pipeline with wax deposition.....	1
Figure 2: Plot of experimental heats of melting for paraffins ($C_1 - C_{21}$).	18
Figure 3: Flow diagram of project	21
Figure 4: Algorithm for calculating the wax mass percent precipitated.....	22
Figure 5: Wax precipitation against temperature for crude oil A	29
Figure 6: Wax precipitation against temperature for crude oil B	29
Figure 7: Wax mass percent against temperature for crude oil A	31
Figure 8: Wax mass percent against temperature for crude oil B.....	31
Figure 9: Wax amount against temperature for crude oil A	33
Figure 10: Wax amount against temperature for crude oil B	33
Figure 11: Wax mass percent against temperature for crude oil A with and without solid-solid transition	35
Figure 12: Wax mass percent against temperature for crude oil B with and without solid-solid transition	35
Figure 13: Comparison of model for crude oil A	37
Figure 14: Comparison of model for crude oil B	38

LIST OF TABLES

Table 1: Experimental and calculated cloud point temperature	8
Table 2: Experimental WAT data and model predictions for crude oils.....	9
Table 3: Solubility Parameters of paraffinic C_{7+} Components.	15
Table 4: Experimental and Calculated Heat Capacity Differences between Liquid and Solid.....	16
Table 5: Measured and calculated enthalpy of Liquid-solid transition.	19
Table 6: Crude oil A compositional characterization	25
Table 7: Crude oil B compositional characterization	26
Table 8: Experimental results and model predictions for crude oil A.....	37
Table 9: Experimental results and model predictions for crude oil B	38

CHAPTER 1

INTRODUCTION

1.1 Background of Study

Crude oil is a hydrocarbon mixture consists of aromatics, paraffins, asphaltenes, and many other compounds. During crude oil production from reservoir to surface, temperature of crude oil decreases to below the cloud point or also known as Wax Appearance Temperature (WAT), this will cause the heavy component like paraffin wax to precipitate and deposit on the pipe wall [1].

Paraffin wax is a hydrocarbon component consists of normal alkanes, cycloalkanes, isoalkanes and aromatic materials. The wax crystals will affect the flow of crude in the pipelines and change the flow behavior from Newtonian to non-Newtonian [2]. This will lead to many problems for the crude oil production and transportation.

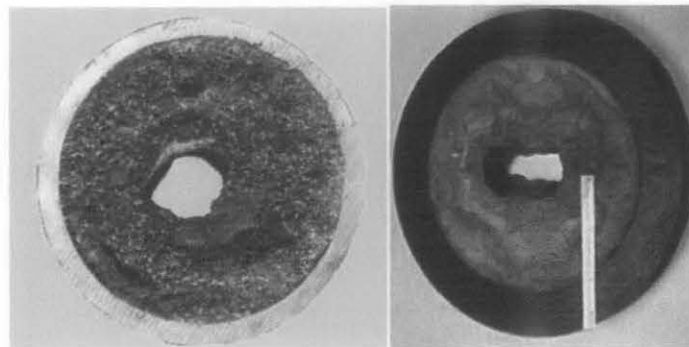


Figure 1: Cross-sectional view of pipeline with wax deposition

Methods have been proposed in the industry to solve the problems related to wax deposition. The common methods are identified in three categories – thermal, mechanical, and chemical [3]. Techniques such as thermal treatment of pipelines, pigging and injection of chemical inhibitors are commonly used to prevent wax buildup [4]. However, the costs of introducing such measures could be reduced if the wax precipitation region is predicted

accurately. Hence, tendency of wax precipitation must be identified at the early stage of crude oil production project.

Many thermodynamic models have been suggested for calculating oil-wax equilibria. From the models a lot of correlations have been applied to predict the thermodynamic parameters, with the purpose to identify the wax formation temperature and wax amount in crude oil. In order to verify the accuracy of the predicted values from the models, the experimental data for wax formation in crude oils has been used to compare the results of these models.

1.2 Problem Statement

Wax precipitation occurs in crude oils may cause problems to the transportation in pipelines, facilities and will result restriction in production [5]. The pipeline internal diameter will be reduced with wax deposition and will become more severe when the whole pipeline is completely blocked. When the pipeline roughness increases, the effective diameter will decrease, thus causes more frequent pigging requirement and potential blockage [2]. This will affect the production rate when the wax deposited in the pipeline causes significant blockage to the flow of crude oil. The blockage of flow will increase energy consumption during pumping of crude oil and thus increase production cost. Moreover, wax deposition in the production system can be very problematic when causing failures to the operating facilities.

The existing thermodynamic models are developed based on regular solution theory to describe the solid-liquid equilibrium during wax formation. However, the solubility parameters and fusion enthalpies of the solid-liquid transition are different for different correlations. This is because crude oils consist of components other than normal paraffins (n-paraffins), such as naphthenic and aromatic components that possess lower fusion enthalpy per weight unit than normal paraffins [6]. The solid-solid transition in the already

formed wax can also affect the model prediction. Thus the thermodynamic parameters need to be revised to produce a more accurate wax model.

This project is significant to develop a wax precipitation model by studying the existing wax models, including the fusion enthalpies, solubility parameters and other parameters. Then the new model with improvement will be presented to increase the accuracy. By knowing the WAT, wax precipitation can be predicted more easily and can enable the work to find out most suitable mitigations to prevent wax formation in the future.

1.3 Objectives

The objectives of this project are as follows:

- (a) To determine the suitable solubility parameters, fusion enthalpy and fusion temperature using the liquid-solid and solid-solid transition.
- (b) To develop a thermodynamic model to predict the Wax Appearance Temperature (WAT) and wax amount.
- (c) To compare the results with the available existing model.

1.4 Scope of Study

The scope of study for this project is to study the existing thermodynamic models so to figure out the weaknesses of the models, and propose an appropriate model for wax precipitation. Generally, the change of temperature, pressure and oil-gas composition can cause heavy paraffin to precipitate as wax in the crude oil. However, predicting the wax appearance point at which the first solid wax is detected can be crucial in production facilities design to prevent wax problems.

In this study, parameters of wax models will be analyzed to produce an improved model to predict wax formation. Later on the results obtained can be compared with the

calculated data from the existing models and experimental results. Computer software such as MATLAB will be used to develop the model. Before hand the properties of wax and the conditions for wax formation must be understood well.

1.5 Relevancy of the Project

This project is related to the crude oil production at which wax precipitation is the problem for crude oil transportation and pipeline integrity. The precipitation of wax is a thermodynamic equilibrium phenomenon and wax properties are very much related to chemical studies.

1.6 Feasibility of Project

This project is feasible by considering several important aspects. The project is targeted to be completed within two semesters or one year time. In the first semester literature review is carried out to gain deeper understanding on the related study. Meanwhile in the second semester, it is scheduled to proceed with the model analysis using software and other tools to achieve the objectives of the project. Subjects taken such as *Introduction to Thermodynamics* and *Chemical Engineering Thermodynamics* are useful for this project. Moreover, no financial assistance is required as the analysis is carried out using available software and spreadsheets while study information is abundantly available online and in the information resource centre.

CHAPTER 2

LITERATURE REVIEW

2.1 Physical Properties of Wax

The properties of wax can be described by hydrocarbon properties since it is formed by hydrocarbon compound. The boiling points of normal hydrocarbons rise with the increase of molecular weight due to the increased attraction between molecules. Isomer structures or branching of the hydrocarbon chain will lower the boiling point [5]. This happens when the magnitude of the transient dipole (London forces) is decreased and the closeness of molecules to each other will also decrease.

Melting point profiles have less regularity compared to boiling point profiles. Melting points depend on how well the molecule fits into a crystal lattice, thus branching determines the effectiveness of the structures of molecules will have higher melting point [5]. Thus, different components other than normal paraffins appear in the crude oils will affect the temperature that wax precipitation will occur.

Wax crystals can be recognized in various geometries, such as cubes, rods, prisms, pentagons, octagons, hexagons, rhomboids and pyramids [5]. Since the geometry of the crystals is determined by the interaction between solute and solvent, thus it is a function of the composition of solute, solvent and physical conditions of the system.

2.2 Molecular Diffusion, Brownian Diffusion, Shear Dispersion and Gravity Settling

In offshore pipeline, the temperature at the center of the pipeline is the hottest while the temperature near the pipe wall is the coldest [1]. This radial temperature gradient will form a concentration gradient of wax in the oil. Thus there will be a mass transfer of wax from the center of the pipe to pipe wall by molecular diffusion.

When the waxy crystals are suspended in oil, they will be bombarded continually by thermally agitated oil molecules. The collisions will lead to random Brownian movements of the suspended particles [8]. Hence Brownian diffusion may also contribute to the wax precipitation.

Flow in pipeline can be considered as a shear field with shear flow, each particle passes and interacts with other particles [2]. The multi-particle interactions will occur in the oil when the particle concentration is high. These particle collisions will lead to shear dispersion of particles that are in interaction.

Wax crystals are denser than the oil medium so would settle and deposit on the bottom of the pipelines. However, mathematical studies show that shear dispersion most likely disperse the settled solids in pipeline flow, so the effect of gravity settling on wax deposition would be neglected [2]. Generally, not much information is available about this mechanism and its significance in wax deposition.

2.3 Mechanism of Paraffin Wax Crystallization

Crystallization is the process of ordered solid structure production from disordered phase [7]. This process involves two distinct stages namely nucleation and growth. The n-paraffins are flexible hydrocarbon molecules and tend to cluster together upon cooling and precipitate to form stable wax solid. Meanwhile, the iso-paraffins content side chains which tend to delay the formation of wax nuclei. This will depress the cloud point and form unstable wax solid. On the other hand, the cyclo-paraffins, or naphthenes, are bulky and tend to disturb the wax nucleation and growth processes. Hence the wax crystals from naphthenes are the least stable saturates. Aromatics are known to be adequate solvents for wax. Impurities usually induce wax nucleation and tend to lower the energy barrier for forming the critical wax nucleus [7].

Since the structures of the hydrocarbon molecules do affect the formation of wax, thus the molecular types and components exist in the oil must be taken into consideration while performing the thermodynamic modeling. Besides, liquid-solid phase transition, solid-solid transition or other characteristics in the oil also can be considered. The parameters which are affected by the liquid-solid phase transition such as solubility parameters, heat capacity and enthalpy of fusion are described in the following sections.

2.4 Thermodynamic Models

In 1986, Won [9] presented a thermodynamic model for predicting wax phase boundaries. The Soave Redlich Kwong equation of state was used for vapor-liquid equilibrium calculations. Meanwhile a modified regular solution approach was used for solid-liquid equilibrium calculations, where the activity coefficients were calculated using solubility parameters of individual components. The fusion temperature and enthalpy were correlated to molecular weight using experimental data mainly for pure n-paraffins with odd carbon numbers. The limitations of the model include inconsistency in description of liquid phase as equation of state is used for vapor-liquid equilibrium while activity coefficient is applied for solid-liquid equilibrium.

Pedersen et al. [6] in 1991 presented a wax model as modifications to the Won's approach. A modified regular solution was applied to both the liquid and solid phases. Fusion properties and heat capacities for pure compound were adjusted to be similar with measured data for North Sea oils. The problem of this model is that it uses unreliable values for fusion properties and heat capacity. The approach proposed led to an overestimation of wax phase boundary temperatures.

In 1996, LiraGaleana et al. [10] presented a wax model that a multi-pure-solid approach was used for description of wax solids. The idea was that wax solids consist of multiple solid phases, and each solid phase was a pure compound. The Peng Robinson equation of state was used for calculating fugacity in the liquid and vapor phases. Table

below shows the comparison between experimental and calculated cloud point temperatures for all the mixtures considered by LiraGaleana et al. [10]

Table 1: Experimental and calculated cloud point temperature

Oil No.	Experimental Temperature (K)	Calculated Temperature (K)	Experimental – Calculated (K)
1	304.15	305.9	-1.75
2	312.15	311.8	0.35
5	313.15	312.4	0.75
8	311.15	308.2	2.95
10	314.15	316.0	-1.85
11	295.15	299.3	-4.15
12	305.15	301.2	3.95
15	308.15	309.5	-1.35

The comparison shows that the calculated values give positive and negative deviations with respect to the experimental values. Simple stability test can be used to determine the number and identity of the potential precipitation phases. Application of this method proposes that the precipitated waxy materials consist of high molecular weight hydrocarbon, which the average carbon atom numbers more than 25. Studies on crystal structures reveal that the miscibility of n-paraffins in a solid state depends strongly on differences in molecular sizes. Thus, assumptions of the multi-pure-solid approach are not consistent with real wax crystal behavior especially for systems consisting of compounds with similar molecular sizes.

In 2006, Chen and Zhao [11] presented a thermodynamic model where solid-solid transition is used to explain the multi-solid phase behavior of waxes before melting. This model is developed by considering the odd and even carbon numbers in mixtures. The number of carbon number is important in predicting the crystal structure. This approach also used in a number of correlations for obtaining the fusion enthalpy to predict wax formation temperature. The calculated values from the model were compared to the WAT of selected hydrocarbon mixtures based on the experimental data from Leelavanichkul et al. [12]

Table 2: Experimental WAT data and model predictions for crude oils

Sample	Experimental Results	Leelavanichkul Model	Deviation	Chen and Zhao's Model	Deviation
Crude oil A	298.2 K	298.6 K	0.4 K	301.3 K	3.1 K
Crude oil B	295.2 K	293.4 K	-1.8 K	295.4 K	0.2 K
Crude oil C	294.2 K	296.0 K	1.8 K	297.8 K	3.6 K

The above values show that the correlations proposed by Chen and Zhao [11] are slightly higher than that predicted by Leelavanichkul et al. [12] The temperature of wax deposition in pipeline may be higher due to some conditions such as the roughness and presence of nucleation site at pipeline wall.

Reza Dalirsefat and Farzaneh Feyzi [13] in 2007 developed a thermodynamic model for wax precipitation using an approach on vapor and liquid phase fugacity. The model calculates the vapor and liquid phase fugacities using the Modified Peng Robinson (MPR) equation of state. It is discussed that there are two methods to solve equilibrium problems. The first method is using an approach of Equation of States (EOS) together with activity coefficient while the second method is only using EOS. The multi-solid model is modified by considering the existence of vapor phase which is in equilibrium with the liquid and some solid phases. The number of solid phases is determined using stability analysis. Meanwhile, PNA analysis for wax precipitation is used to consider the differences in the properties of paraffins, naphthenes and aromatics. The modifications have improved the prediction of WAT as compared to the previous methods. The prediction for the amount of precipitated wax is better than Pedersen et al. [7] model and comparable to LiraGaleana et al. [10] model.

2.5 Thermodynamic Equations

Since the wax precipitation is a process of transition of liquid to solid wax crystal, thus understanding in solid-liquid equilibrium (SLE) is essential. In the development of the related thermodynamic models, the information from this SLE offers highly accurate estimation of parameters such as the fugacity which will be helpful in developing the thermodynamic model.

Fugacity is a measure of chemical potential in the form of 'adjusted pressure'. The phase with the lowest fugacity is most favorable as the Gibbs free energy is also the lowest. Multiphase phases at the same temperature and pressure are in equilibrium when the fugacity of each constituent species is the same in all phases [14].

This section shows the methods to obtain the thermodynamic model by considering the liquid-solid transition. At thermodynamic equilibrium between liquid phase (oil) and solid phase (wax), the fugacity of component i in oil phase which is equal to fugacity in solid phase can be expressed as:

$$f_i^L = f_i^S \quad (1)$$

The liquid phase fugacity of component i can be represented by:

$$f_i^L = \gamma_i^L x_i^L f_i^{\circ L} \exp\left(\int_0^P \frac{V_i^L dP}{RT}\right) \quad (2)$$

where γ_i^L is the activity coefficient of component i in liquid phase, x_i^L the mole fraction of component i in the liquid phase, $f_i^{\circ L}$ the standard state fugacity of component i in the liquid phase, V_i^L the molar liquid volume of component i , P the pressure, R the gas constant, and T the temperature. Similarly, solid phase fugacity will be:

$$f_i^S = \gamma_i^S x_i^S f_i^{\circ S} \exp\left(\int_0^P \frac{V_i^S dP}{RT}\right) \quad (3)$$

By combining equations above,

$$\frac{x_i^S}{x_i^L} = \frac{\gamma_i^L f_i^{\circ L}}{\gamma_i^S f_i^{\circ S}} \exp\left(\int_0^P \frac{V_i^L - V_i^S}{RT} dP\right) \quad (4)$$

By assuming liquid and solid phase molar volumes have very little difference under low and moderate pressures, this expression will be simplified to:

$$\exp\left(\int_0^P \frac{V_i^L - V_i^S}{RT} dP\right) = 0$$

$$\frac{x_i^S}{x_i^L} = \frac{\gamma_i^L f_i^{\circ L}}{\gamma_i^S f_i^{\circ S}} \quad (5)$$

From the general thermodynamic relation:

$$\Delta G = \Delta H - T\Delta S \quad (6)$$

and the molar change in Gibbs free energy with transition from liquid to solid:

$$\Delta G_{ad} = RT \ln\left(\frac{f_i^{\circ S}}{f_i^{\circ L}}\right) \quad (7)$$

Together with the enthalpy change of liquid-solid phase transition at temperature T , lower than normal melting temperature, T^f , and considering components other than normal paraffins:

$$\Delta H_{ad} = -\Delta H^f + \int_T^{T^f} (C_p^L - C_p^S) dT \quad (8)$$

where ΔH^f is the heat of fusion, C_p^L is the liquid phase heat capacity and C_p^S is the solid phase heat capacity, while the entropy change associated with liquid-solid transition is:

$$\Delta S_{ad} = \frac{-\Delta H^f}{T^f} + \int_T^{T^f} \frac{C_p^L - C_p^S}{T} dT \quad (9)$$

By combining equation (5) to (9), the ratio of mole fractions for solid phase and liquid phase can be derived.

$$\frac{x_i^S}{x_i^L} = \frac{\gamma_i^L}{\gamma_i^S} \exp\left(\frac{\Delta H_i^f}{RT} \left(1 - \frac{T}{T_i^f}\right) - \frac{1}{RT} \int_T^{T_i^f} (C_p^L - C_p^S) dT + \frac{1}{R} \int_T^{T_i^f} \frac{C_p^L - C_p^S}{T} dT\right) \quad (10)$$

2.5.1 Activity Coefficients

The activity coefficient for solid and liquid phases can be written based on modified regular solution theory with solubility parameters used by Won [9]:

$$\ln \gamma_i^L = \frac{V_i^L(\delta_m^L - \delta_i^L)^2}{RT} \quad \ln \gamma_i^S = \frac{V_i^S(\delta_m^S - \delta_i^S)^2}{RT} \quad (11)$$

$$\delta_m^L = \sum \Phi_i^L \delta_i^L \quad \delta_m^S = \sum \Phi_i^S \delta_i^S \quad (12)$$

$$\Phi_i^L = \frac{x_i^L V_i^L}{\sum x_i^L V_i^L} \quad \Phi_i^S = \frac{x_i^S V_i^S}{\sum x_i^S V_i^S} \quad (13)$$

where δ_i^L and δ_i^S are solubility parameters of component i in the liquid and solid states, respectively. The term Φ_i^L is the volume fraction of component i in the liquid phase, and Φ_i^S is the volume fraction of component i in the solid phase. The average solubility parameters δ_m^L and δ_m^S of liquid and solid phases are found as volumetric mean values.

Meanwhile the terms V_i^L and V_i^S are the molar volumes (cm^3/mol) of component i in liquid and solid which can be obtain from the molecular weight, MW_i and liquid phase density, d_i^L at 298.15K:

$$V_i^L = V_i^S = \frac{MW_i}{d_i^L} \quad (14)$$

The liquid phase density d_i^L at 25 °C can be calculated by using the correlation proposed by Won [9] for paraffin components based on molecular weight:

$$d_{i,25}^L = 0.815 + 0.06272 \times 10^{-4} MW_i - \frac{13.06}{MW_i} \quad (15)$$

Liquid phase density for components other than paraffin can be obtained from Leelavanichkul et al. [12] correlations,

For naphthenic components:

$$d_{i,25}^L = 0.865 + 0.06272 \times 10^{-4} MW_i - \frac{13.06}{MW_i} \quad (16)$$

For aromatic components:

$$d_{i,25}^L = -0.03 \ln MW_i + 1.02 \quad (17)$$

2.5.2 Liquid and Solid Phase Solubility Parameters

The regular solution theory presented by Won [9] model has given the solubility parameters of hydrocarbons up to C₄₀. However these values of solubility parameters are based on the literature values for normal paraffins. Besides normal paraffins, branched paraffins such as naphthenes, and aromatics also need to be taken into consideration. Naphthenes and aromatics are assigned values of the solubility parameters which are 20 percent higher than those of paraffins [6].

The solubility parameters in liquid state can be calculated from a correlation proposed by Riazi and Al-Sahhaf [15] for paraffin components in crude oils:

$$\delta_i^L = 8.6 - \exp(2.219195 - 0.54907 MW_i^{0.3}) \quad (18)$$

The solubility parameters for other compounds are estimated by using correlations from Leelavanichkul et al. [12]

For naphthenic components:

$$\delta_i^L = 8.7 - \exp(2.219195 - 0.54907 MW_i^{0.3}) \quad (19)$$

For aromatic components:

$$\delta_i^L = 8.8 - \exp(2.219195 - 0.54907MW_i^{0.3}) \quad (20)$$

The solubility parameters of component i in solid solution can be expressed as [12]

$$\delta_i^S = \left(\frac{\Delta H_i^f}{V_i} + \delta_i^{L2} \right)^{0.5} \quad (21)$$

Meanwhile, the equations that suggested by Pedersen et al. [6] for paraffinic and naphthenic part of a C_{7+} fraction are

$$\delta_i^L = 7.41 + 0.5914(\ln C_N - \ln 7) \quad (22)$$

$$\delta_i^S = 8.50 + 5.763(\ln C_N - \ln 7) \quad (23)$$

Table 3: Solubility Parameters of paraffinic C₇₊ Components Used in the Model of Won and Modified Model presented by Pedersen et al. [6]

Component	Won		Pedersen et al.	
	δ_L	δ_S	δ_L	δ_S
C7	7.41	8.50	7.41	8.50
C8	7.53	8.78	7.49	9.27
C9	7.63	9.00	7.56	9.95
C10	7.71	9.17	7.62	10.60
C11	7.78	9.32	7.68	11.10
C12	7.83	9.44	7.13	11.60
C13	7.88	9.55	7.78	12.10
C14	7.92	9.64	7.82	12.50
C15	7.96	9.72	7.86	12.90
C16	7.99	9.79	7.90	13.30
C17	8.02	9.86	7.93	13.60
C18	8.05	9.92	7.91	13.90
C19	8.07	9.97	8.00	14.30
C20	8.09	10.00	8.03	14.60
C21	8.11	10.10	8.06	14.80
C22	8.13	10.10	8.09	15.10
C23	8.15	10.10	8.11	15.40
C24	8.17	10.20	8.14	15.60
C25	8.18	10.20	8.16	15.80
C26	8.20	10.30	8.19	16.10
C27	8.21	10.30	8.21	16.30
C28	8.22	10.30	8.23	16.50
C29	8.24	10.30	8.25	16.70
C30	8.25	10.40	8.27	16.90
C31	8.26	10.40	8.29	17.10
C32	8.27	10.40	8.31	17.30
C33	8.28	10.40	8.33	17.40
C34	8.29	10.40	8.34	17.60
C35	8.30	10.50	8.36	17.80
C36	8.31	10.50	8.38	17.90
C37	8.32	10.50	8.39	18.10
C38	8.33	10.50	8.41	18.20
C39	8.34	10.50	8.43	18.40
C40	8.35	10.60	8.44	18.50

The solubility parameters suggested by Won and the estimated values which considering paraffinic and naphthenic components are shown in table above. The liquid phase solubility parameters are almost identical while the solid phase solubility parameters are higher than those suggested by Won. Components with similar molecular weight could have difference in the molecular structures either in naphthenic or aromatic compounds which can affect the solubility [6].

2.5.3 Liquid and Solid Phase Heat Capacity

The heat capacity difference due to the liquid-solid phase transitions was shown by Pedersen et al. [6] in 1991. The equation of heat capacity difference based on molecular weight and temperature is:

$$\Delta C_{pi} = 0.3033MW_i - 4.635 \times 10^{-4} MW_i T \quad (24)$$

Table 4: Experimental and Calculated Heat Capacity Differences between Liquid and Solid Phases at 250 K [6]

Compound	ΔC_p , cal/(mol K)	
	Experimental	Calculated
C8	9.9	21.4
C16	28.7	42.3
C25	43.2	65.9
C33	63.4	86.9

The heat capacities of the liquid-solid phase are different from the measured values for normal paraffins. This can be caused by the fact that the oils contain other types of components other than normal paraffins. This will affect the difference of heat capacity of liquid-solid phase for hydrocarbon chain heavier than C₇₊.

2.5.4 Fusion Enthalpy

The fusion enthalpy of the normal paraffins is given by Won's model as [9]

$$\Delta H_i^f = 0.1426MW_iT_i^f \quad (25)$$

However, the existence of isoparaffins in the oils can be considered by modifying the fusion enthalpy for normal paraffins. The fusion temperature proposed by Won [9]:

$$T_i^f = 374.5 - 0.02617MW_i + \frac{20172}{MW_i} \quad (MW_i \leq 450g/mol) \quad (26)$$

$$T_i^f = 411.4 - \frac{32326}{MW_i} \quad (MW_i \geq 450g/mol) \quad (27)$$

The fusion enthalpies of n-alkanes have different correlations according to the number of carbon atoms and the odd or even carbon number in the chain proposed by Chen and Zhao [11],

For n-paraffins with odd carbon number:

$$7 < C_n < 21 \quad \Delta H_i^f = 0.5754MW_iT_i^f \quad (28)$$

For n-paraffins with even carbon number:

$$8 \leq C_n < 22 \quad \Delta H_i^f = 0.8064MW_iT_i^f \quad (29)$$

For n-paraffins with all carbon number:

$$21 \leq C_n < 38 \quad \Delta H_i^f = 0.4998MW_iT_i^f \quad (30)$$

$$C_n \geq 38 \quad \Delta H_i^f = 0.6741MW_iT_i^f \quad (31)$$

Broadhurst [16] also studies on the solid phase behavior of the normal paraffins to obtain the effects of odd and even carbon number to the fusion enthalpies. The following figure shows the results obtained by the author.

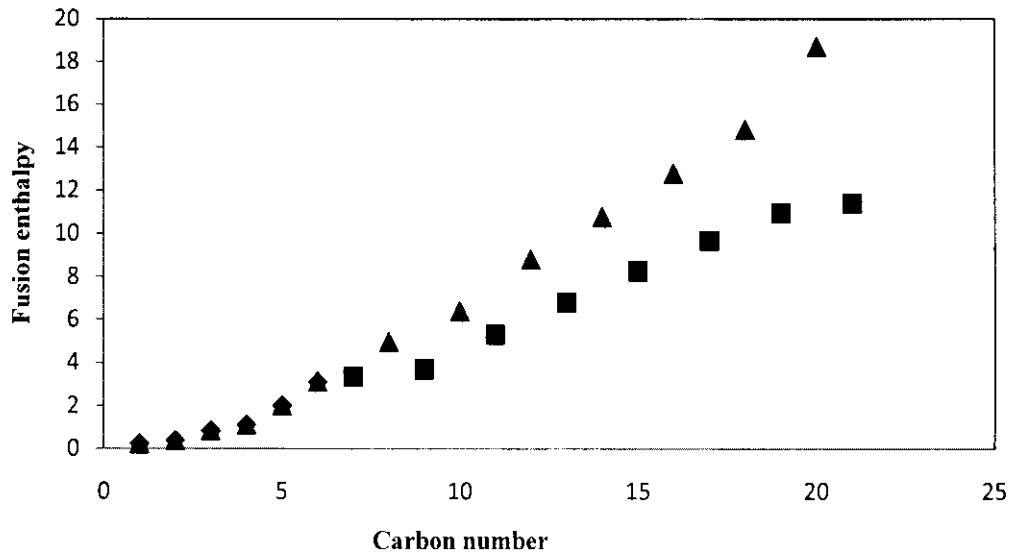


Figure 2: Plot of experimental heats of melting for paraffins ($C_1 - C_{21}$). Symbols: ■, Odd; ▲, Even; ◆, C7-

From Figure 2, even carbon number components in the oil mixture will give higher values to the fusion enthalpies. Meanwhile the odd carbon number paraffins have smaller values of fusion enthalpy. This is due to the difference of the molecular structure of the odd and even carbon number in the element. When the carbon number is increasing, the fraction of n-paraffins present in the oil mixture is decreasing and thus will affect the fusion enthalpy. This gives significant effects to the measurement of WAT if it is not taken into consideration.

Pedersen et al. [6] has also presented the measured and calculated results for the enthalpy change associated with the wax precipitation. The measured results are from the differential scanning calorimetry measurements to be compared with the calculated values.

When the temperature of oil is lower than WAT, the solid phases of all n-paraffins with more than 9 carbon atoms in the chain consist of four distinct crystal structures namely hexagonal, triclinic, monoclinic and orthorhombic [16]. These different structures of molecules can affect the fusion enthalpies of the wax.

Table 5: Measured and calculated enthalpy of Liquid-solid transition by Pedersen et al. [6]

Enthalpy change, cal/g of wax			
Oil no.	Measured	Calculated	Measured/calculated
2	43.3	10.9	4.0
3	40.6	9.3	4.3
4	66.3	12.3	5.4
5	56.1	8.3	6.8
6	52.5	7.9	6.7
7	45.7	7.6	6.0
8	54.1	9.9	6.9
9	37.8	7.7	5.0
10	58.8	10.2	5.9
12	71.2	8.0	7.0
14	43.3	7.7	5.6
15	56.6	8.3	6.8
16	42.5	11.1	3.8
17	28.0	7.3	3.9

As shown in the Table 5 above, the calculated values are smaller as compared to the measured values. The enthalpy change of liquid-solid transition is fairly small as compared with the pure component melting enthalpies. Somehow the remaining enthalpy changes can be contributed by phase transitions taking place in the already formed wax [6]. The calculations do not take into account phase transitions in the already formed wax. This is the reason why the calculated enthalpy changes are very much smaller than the values measured experimentally.

Generally, the model to predict the wax formation has been established as shown by Equation (10). The suitable parameters of this equation need to be identified to produce a useful model for predicting wax precipitation. The useful factors to be considered are the solubility parameters, enthalpy of fusion, heat capacity of liquid-solid phase transition, together with the required factors, such as activity coefficient, volume fraction and temperature of fusion. Further methodology will be discussed in the following part for the model.

2.5.5 Solid-solid Transition

All the correlations above are useful to be applied for the liquid-solid transition during the precipitation of wax. However, considering the liquid-liquid transition characteristics in the already formed wax with several third-order polynomial functions [11] can improve the accuracy of the model:

For n-paraffins with odd carbon number:

$$9 \leq C_n \leq 43$$

$$T_i^t = 0.0039C_n^3 - 0.4249C_n^2 + 17.2812C_n + 93.1012 \quad (32)$$

$$\Delta H_i^t = 39805.146 - 6180.1417C_n + 347.9015C_n^2 - 4.9602C_n^3 \quad (33)$$

For n-paraffins with even carbon number:

$$22 \leq C_n \leq 42$$

$$T_i^t = 0.0032C_n^3 - 0.3249C_n^2 + 12.7811C_n + 157.1936 \quad (34)$$

$$\Delta H_i^t = 44019.633 - 6181.7767C_n + 348.7432C_n^2 - 4.9661C_n^3 \quad (35)$$

The ratio of mole fractions for solid phase and liquid phase can be revised from Equation (10) to:

$$\frac{x_i^S}{x_i^L} = \frac{\gamma_i^L}{\gamma_i^S} \exp\left(\frac{\Delta H_i^f}{RT}\left(1 - \frac{T}{T_i^f}\right) + \frac{\Delta H_i^t}{RT}\left(1 - \frac{T}{T_i^t}\right) - \frac{1}{RT} \int_T^{T_i^f} (C_p^L - C_p^S) dT + \frac{1}{R} \int_T^{T_i^f} \frac{C_p^L - C_p^S}{T} dT\right) \quad (36)$$

CHAPTER 3 METHODOLOGY

The relevant parameters are to be considered in the formation of wax for liquid-solid transition. This project does not require experimental procedures but computational calculation is needed. MATLAB and MICROSOFT EXCEL are the computer aided software to be used in this project. The procedures to perform this project are shown in figure below:

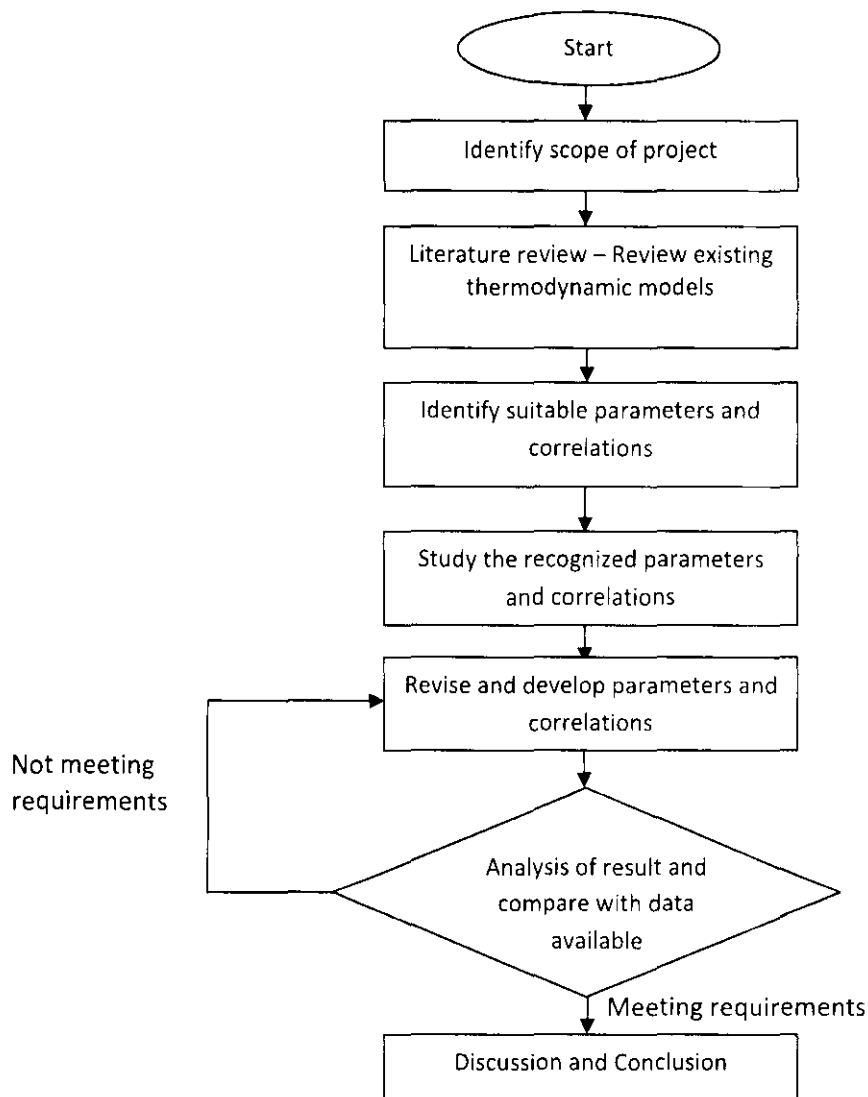


Figure 3: Flow diagram of project

3.1 Computational Processes

The programming steps by using MATLAB with the algorithm used in calculating the wax mass percent precipitated will be as follows:

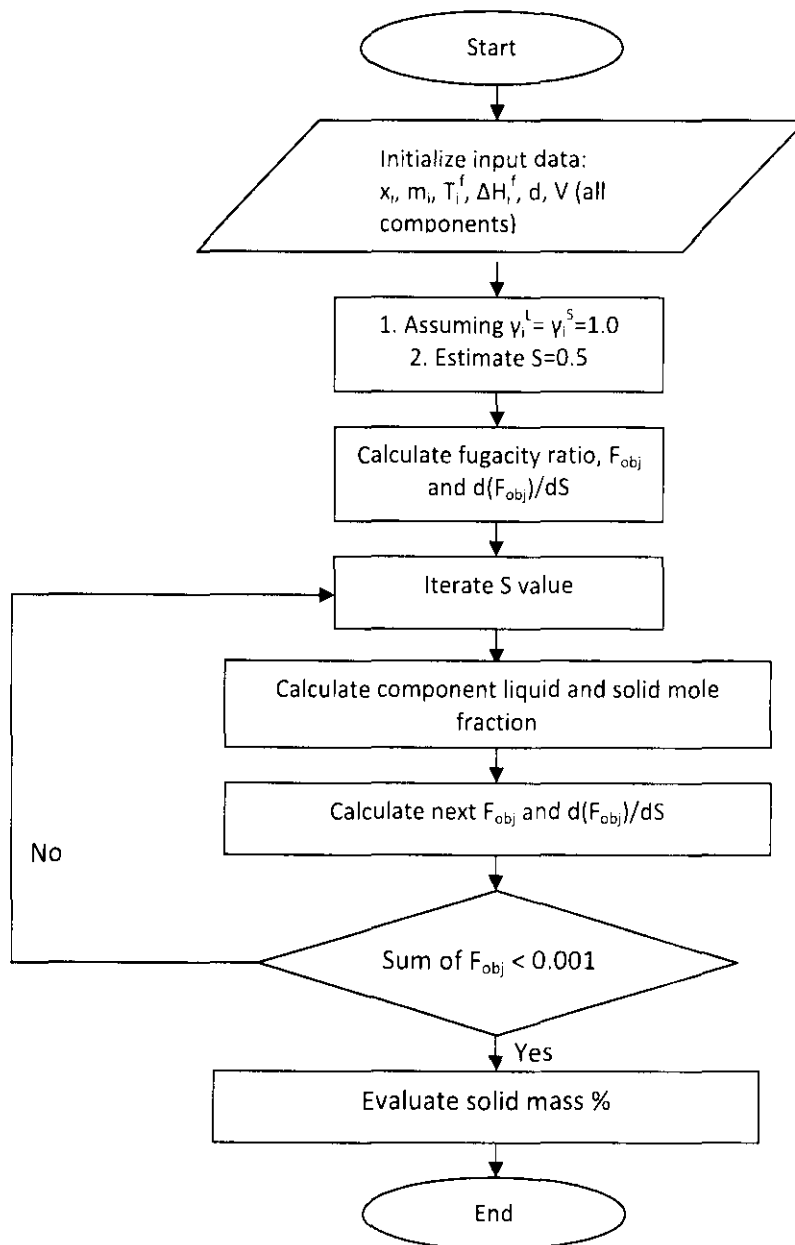


Figure 4: Algorithm for calculating the wax mass percent precipitated [11]

Following is the description of the suggested calculation process above [11]:

- (1) Initialize the system and input data x_i and m_i for each component, including T_i^f , ΔH_i^f , d and V for C_{7-} component.
- (2) For first iteration, estimate first solid mole fraction = 0.5, $\gamma_i^L = \gamma_i^S = 1.0$
- (3) Calculate initial solid liquid equilibrium constant (K^{SL}) objective function and its derivative.
- (4) Calculate next solid phase mole fraction, S .
- (5) Calculate component mole fractions in liquid and solid phases.
- (6) Calculate parameters: molar volumes, volume fractions and solubility parameters for solid and liquid phases.
- (7) Calculate activity coefficients for solid and liquid phases.
- (8) Calculate next K^{SL} objective function and its derivative.
- (9) Check whether the sum of objective function is less than 0.001. If yes, calculate solid mass percent of each component and total mass percent solid. If not, return to (4).

The objective function and its derivative are calculated by the following equations:

$$F_{obj} = \Sigma \left[\frac{x_i (K_i^{SL} - 1)}{1 + S(K_i^{SL} - 1)} \right] \quad (37)$$

$$\frac{d(F_{obj})}{dS} = -\Sigma \left[\frac{x_i (K_i^{SL} - 1)^2}{1 + S(K_i^{SL} - 1)^2} \right] \quad (38)$$

3.2 Gantt Chart

FYP1

Detail / Week	1	2	3	4	5	6	7	8	9	Mid Semester Break	10	11	12	13	14	
Selection of Project Topic	√															
Release of Topics Selection		√														
Proposal			√													
Literature Review			√	√	√	√										
Identify suitable software						√										
Identify general thermodynamic equation of solid-liquid transition						√	√									
Identify density and molar volume							√									
Identify activity coefficient								√	√							
Identify solubility parameters									√			√				
Identify enthalpy of fusion												√	√			
Identify heat capacity of liquid-solid transition														√	√	

FYP2

Detail / Week	1	2	3	4	5	6	7	Mid Semester Break	8	9	10	11	12	13	14	
Modeling of existing models	√	√														
Analysis with existing results & check accuracy		√	√													
Identify weaknesses			√	√												
Modeling with improved parameters					√	√	√			√	√	√				
Analysis with experimental data												√	√			
Finalize improved parameters														√		
Analysis of model															√	√

CHAPTER 4

RESULTS AND DISCUSSION

4.1 Data Gathering

In order to proceed and to access the oil mixture contents, oil mixture samples are required. Two sets of composition and molecular weight of oil mixture are taken from the paper developed by Leelavanichkul et al. [12]

Table 6: Crude oil A compositional characterization

Component	Mol %	MW	Mol %	MW	Mol %	MW
Light fraction						
C1	0.000	16.0				
C2	0.073	30.1				
C3	0.696	44.1				
C4	4.563	58.1				
C5	3.342	72.2				
C6	2.486	82.0				
Solute fraction						
	P		N		A	
C7	5.913	100.2	1.812	96.8	1.609	91.1
C8	4.237	114.2	1.747	110.6	1.766	104.1
C9	3.343	128.3	1.742	124.4	1.883	117.2
C10	2.438	142.3	1.512	138.2	1.711	130.2
C11	1.659	156.3	1.281	152.1	1.523	143.2
C12	1.174	170.3	1.189	165.9	1.555	156.2
C13	1.171	184.4	1.226	179.7	1.673	169.2
C14	0.916	198.4	1.079	193.5	1.678	182.3
C15	0.748	212.4	0.967	207.4	1.665	195.3
C16	0.591	226.4	0.810	221.2	1.466	208.3
C17	0.510	240.5	0.724	235.0	1.349	221.3
C18	0.451	254.5	0.664	248.8	1.338	234.3
C19	0.433	268.5	0.509	262.7	1.305	247.3
C20	0.309	282.5	0.446	276.5	1.219	260.4
C21	0.274	296.6	0.363	290.3	1.100	273.4
C22	0.248	310.6	0.310	304.1	1.046	286.4
C23	0.224	324.6	0.250	318.0	0.941	299.4
C24	0.203	338.6	0.226	331.8	0.853	312.4
C25	0.183	352.7	0.203	345.6	0.766	325.5
	n-alkane		non-n-alkane		aromatic	
C26	0.138	366.7	0.484	377.8	0.445	338.5

C27	0.080	380.7	0.486	392.3	0.352	351.5
C28	0.067	394.7	0.468	406.8	0.352	364.5
C29	0.040	408.8	0.469	421.4	0.337	377.5
C30	0.027	422.8	0.417	435.9	0.300	390.5
C31	0.024	436.8	0.385	450.4	0.293	403.6
C32	0.022	450.8	0.325	465.0	0.256	416.6
C33	0.026	464.9	0.298	479.5	0.246	429.6
C34	0.017	478.9	0.259	494.0	0.221	442.6
C35	0.008	492.9	0.234	508.6	0.202	455.6
C36	0.007	507.0	0.229	523.1	0.193	468.6
C37	0.005	521.0	0.206	537.6	0.183	481.7
C38	0.004	535.0	0.184	552.1	0.170	494.7
C39	0.004	549.0	0.165	566.7	0.162	507.7
C40	0.002	563.1	0.148	581.2	0.148	520.7
C41	0.002	577.1	0.137	595.7	0.138	533.7
C42	0.002	591.1	0.119	610.3	0.140	546.8
C43	0.001	605.1	0.114	624.8	0.121	559.8
C44	0.001	619.2	0.097	639.3	0.117	572.8
C45	0.001	633.2	0.093	653.9	0.110	585.8
C46	0.001	647.2	0.077	668.4	0.109	598.8
C47	0.001	661.2	0.073	682.9	0.095	611.8
C48	0.001	675.3	0.066	697.4	0.093	624.9
C49	0.001	689.3	0.062	712.0	0.081	637.9
C50	0.000	703.3	0.053	726.5	0.079	650.9
C50+	2.753	713.0				

Table 7: Crude oil B compositional characterization

Component	Mol %	MW	Mol %	MW	Mol %	MW
Light fraction						
C1	0.050	16.0				
C2	0.000	30.1				
C3	1.001	44.1				
C4	1.829	58.1				
C5	2.335	72.2				
C6	3.846	82.0				
Solute fraction						
	P		N		A	
C7	5.850	100.2	1.765	96.8	1.360	91.1
C8	6.809	114.2	2.803	110.6	2.672	104.1
C9	4.613	128.3	2.323	124.4	2.394	117.2
C10	3.028	142.3	1.902	138.2	2.052	130.2

C11	2.105	156.3	1.575	152.1	1.761	143.2
C12	1.566	170.3	1.407	165.9	1.668	156.2
C13	1.279	184.4	1.304	179.7	1.717	169.2
C14	1.036	198.4	1.201	193.5	1.771	182.3
C15	0.798	212.4	1.022	207.4	1.634	195.3
C16	0.550	226.4	0.807	221.2	1.428	208.3
C17	0.518	240.5	0.772	235.0	1.332	221.3
C18	0.299	254.5	0.466	248.8	0.890	234.3
C19	0.356	268.5	0.538	262.7	1.065	247.3
C20	0.292	282.5	0.471	276.5	1.028	260.4
C21	0.241	296.6	0.404	290.3	0.994	273.4
C22	0.213	310.6	0.330	304.1	0.886	286.4
C23	0.209	324.6	0.299	318.0	0.859	299.4
C24	0.176	338.6	0.255	331.8	0.756	312.4
C25	0.162	352.7	0.236	345.6	0.743	325.5
		n-alkane	non-n-alkane		aromatic	
C26	0.090	366.7	0.494	377.8	0.475	338.5
C27	0.041	380.7	0.358	392.3	0.342	351.5
C28	0.039	394.7	0.344	406.8	0.331	364.5
C29	0.024	408.8	0.333	421.4	0.303	377.5
C30	0.021	422.8	0.292	435.9	0.291	390.5
C31	0.015	436.8	0.265	450.4	0.257	403.6
C32	0.012	450.8	0.223	465.0	0.241	416.6
C33	0.013	464.9	0.193	479.5	0.225	429.6
C34	0.014	478.9	0.167	494.0	0.196	442.6
C35	0.007	492.9	0.154	508.6	0.188	455.6
C36	0.004	507.0	0.144	523.1	0.180	468.6
C37	0.003	521.0	0.131	537.6	0.160	481.7
C38	0.002	535.0	0.119	552.1	0.150	494.7
C39	0.003	549.0	0.099	566.7	0.140	507.7
C40	0.001	563.1	0.091	581.2	0.129	520.7
C41	0.001	577.1	0.080	595.7	0.120	533.7
C42	0.001	591.1	0.074	610.3	0.114	546.8
C43	0.001	605.1	0.066	624.8	0.102	559.8
C44	0.001	619.2	0.062	639.3	0.095	572.8
C45	4.00E-4	633.2	0.052	653.9	0.091	585.8
C46	4.31E-4	647.2	0.050	668.4	0.083	598.8
C47	2.05E-4	661.2	0.046	682.9	0.076	611.8
C48	2.87E-4	675.3	0.041	697.4	0.072	624.9
C49	0.000	689.3	0.040	712.0	0.064	637.9
C50	0.000	703.3	0.035	726.5	0.062	650.9
C50+	1.764	825.5				

The tables above, Table 6 and Table 7 show that there are over hundred pseudocomponents in the crude oil. All the pseudocomponents are determined based on carbon number ranges and hydrocarbon group types. The light fractions (C7-) are attributed to single carbon number. Every carbon number of the solvent fractions (C7-C25) is categorized into paraffin, naphthene and aromatic fractions. Meanwhile the other solute fractions (C26-C50) are classified as saturate (n-alkane, non-n-alkane) and aromatic fractions. Finally the heavy fractions are lumped into one C50+ fraction. Since crude oils content thousands of different components, all of the components cannot be identified. Thus the lumping categorization is essential for predicting the thermodynamic properties of the crude oils.

4.2 Modeling Results

Based on the crude samples collected, the wax precipitation of the samples has been modeled, at which the parameters including fusion temperature, T_i^f , fusion enthalpy, H_i^f of solid-liquid transition, and solubility parameters, δ_i are used in MATLAB software. The amount of wax in weight percent (wt %) can be obtained from the model by varying the values of temperature. This model is convenient to determine the amount of wax formed at certain temperatures.

The following sections will show the effects of the model parameters to the characteristics of the thermodynamic model. Due to the fact that crude oils consist of thousands of components, the composition will be very difficult to be measured and predicted. Thus, this work is an estimation work at which the parameters and correlations used are helpful to approximate the characteristics of crude oils as temperature changes. Somehow, distinct errors would occur for each estimation or modeling where there are factors that can affect the results. These factors will be discussed later.

4.2.1 Effect of Carbon Number

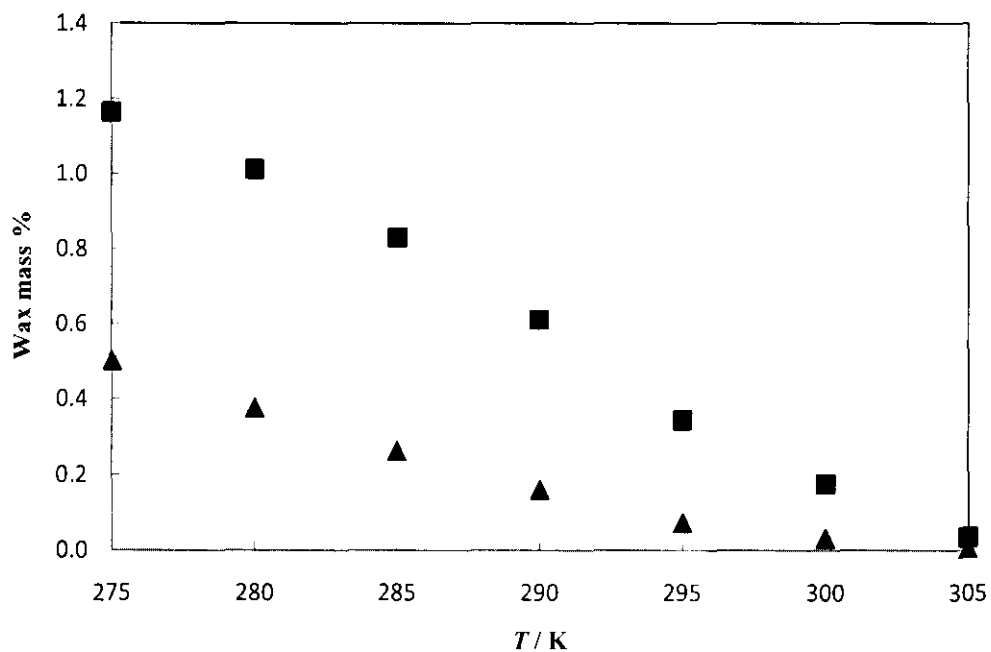


Figure 5: Wax precipitation against temperature for crude oil A. Symbols: \blacksquare , C1-C50; \blacktriangle , C1-C25

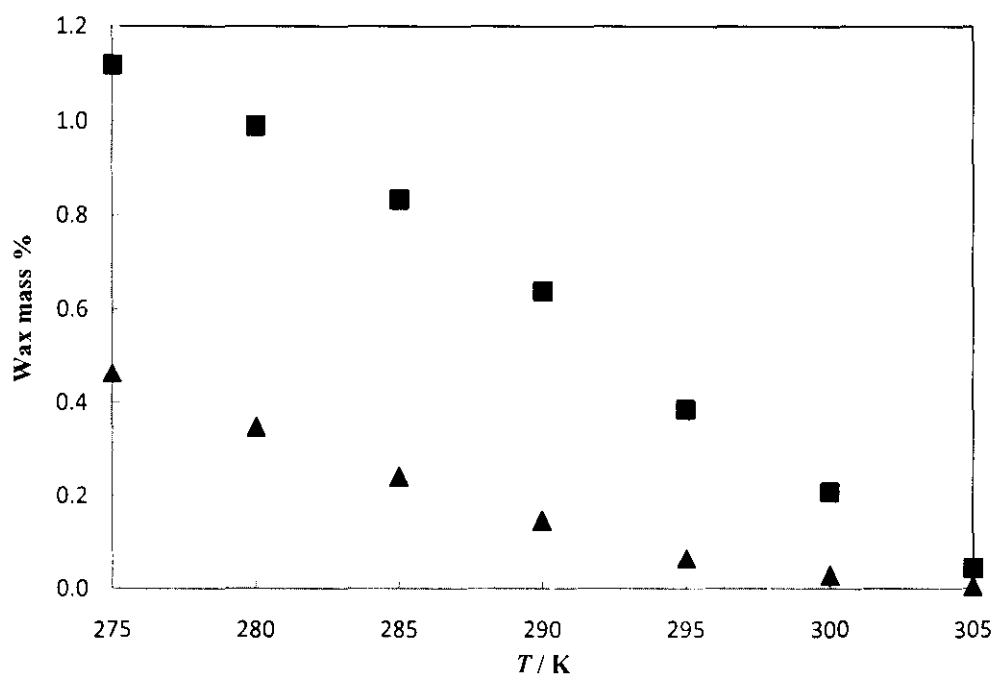


Figure 6: Wax precipitation against temperature for crude oil B. Symbols: \blacksquare , C1-C50; \blacktriangle , C1-C25

The above figures show that the amount of wax precipitated increases as the temperature drops for both crude oil A and B. This is a desired trend and positive results. The results for crude oil A is represented in Figure 5. The curve of C1-C25 shows that the amount of wax percent formed is lower compared to the one of C1-C50. In this case, the amount of wax precipitated at 275K is approximately 0.5 wt % for the model that uses carbon number from C1 to C25. Meanwhile the model that takes more carbon numbers available from the crude sample from C1 to C50, and also lumping the heavy fraction C50+ tends to give more wax, which is nearly 1.2 wt %. This actually explains that the number of carbons being used in the model will significantly affect the accuracy of the prediction of wax amount.

The same condition happens for crude oil B as shown in Figure 6. The trend of the amount of wax formed with respect to temperature proves that the heavy components, typically carbon numbers larger than C25 give more influence to the wax precipitation. This matches with the factor discussed by Broadhurst [16] where solid phases of all n-paraffins with heavy carbon atoms in the chain consist of four distinct crystal structures namely hexagonal, triclinic, monoclinic and orthorhombic that may affect the characteristics of the wax precipitation.

4.2.2 Effect of Fusion Enthalpy

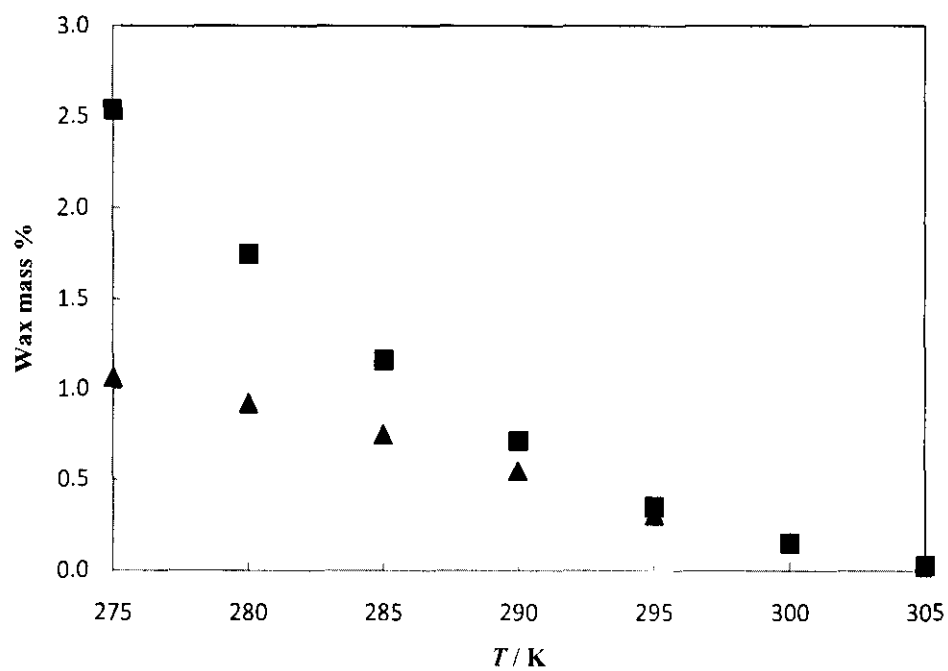


Figure 7: Wax mass percent against temperature for crude oil A. Symbols: \blacksquare , With odd & even C; \blacktriangle , Without odd & even C

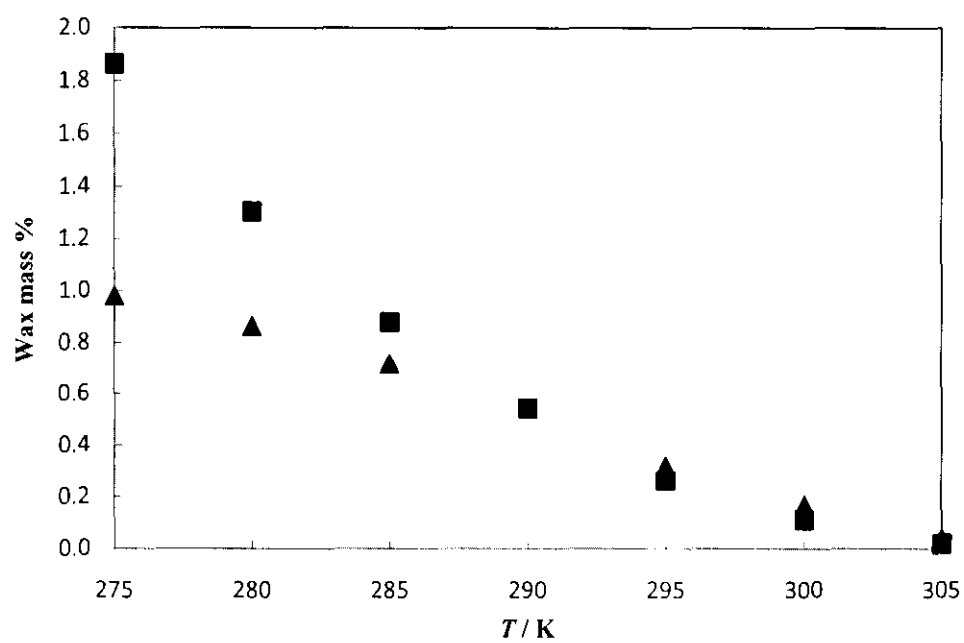


Figure 8: Wax mass percent against temperature for crude oil B. Symbols: \blacksquare , With odd & even C; \blacktriangle , Without odd & even C

From Figure 7 and Figure 8 above, the amount of wax precipitated for the model which is considering different fusion enthalpy correlations for odd and even carbon number is more than the model which uses single equation for the odd and even carbon numbers. The model that does not consider different fusion enthalpy correlations for odd and even carbon numbers will give results with less wax precipitation. This type of model is using the fusion enthalpy as of Equation (25) for all the n-paraffins without differentiating the number of carbon number present.

However, the model with break down of carbon number for fusion enthalpy of n-paraffins as in Equation (28)-(31) gives different amounts. With this categorization, the model gives a significant increase of wax amount as the temperature decreases. In Figure 8, a trend exists at which when the temperature is still high, the amount of wax precipitated from the odd and even carbon number fusion enthalpy correlations could be lower than the wax amount with the single enthalpy equation. However, the wax amount increases drastically as the temperature reduces. This can give serious problem because the big amount of wax would clog the crude transfer pipelines and will lead to many other negative effects. Thus the break down of the odd and even carbon numbers is important for the development of the wax model.

The main reason that leads to the results is the difference of the molecular structure of the odd and even carbon number. When the carbon number increases, the fraction of n-alkanes present in the oil decreases, meanwhile the fraction of components other than n-alkanes increased and thus will affect the fusion enthalpy.

Moreover, the odd and even carbon effect is related to the packing differences of the carbon atoms in the molecules. When the paraffin chains are packed vertically, there is no packing difference for the molecule chains of odd and even numbered molecules. But when the molecules are tilted and come close to each other, only the even paraffins have the symmetry required for equivalent packing of both end groups. If the odd numbered chain is tilted, only one end group of the molecular chain can be packed, but the other end is less

packed as the naturally required symmetry could not be found. Thus their fusion enthalpies are different.

4.2.3 Effect of Solubility Parameters

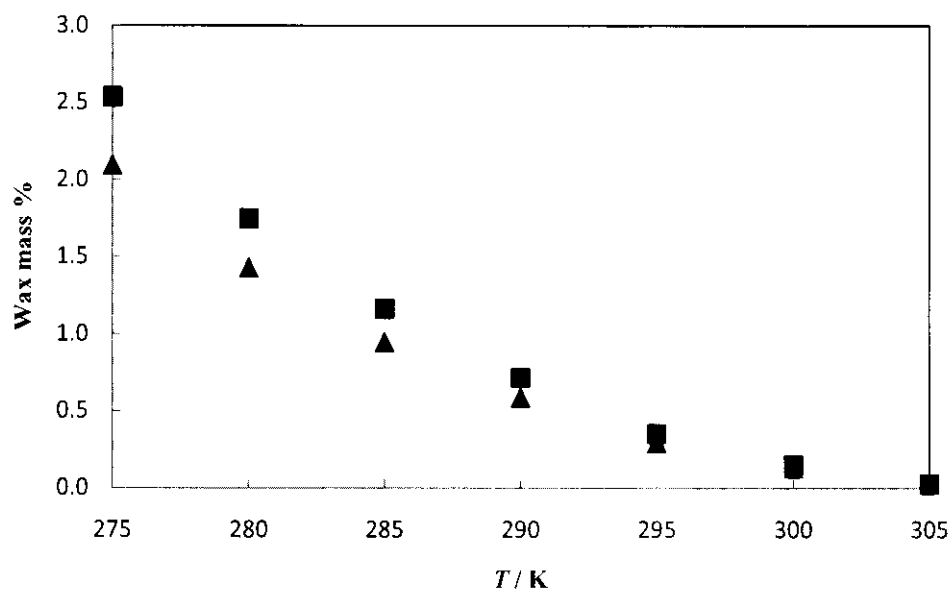


Figure 9: Wax amount against temperature for crude oil A. Symbols:
■, PNA; ▲, Without PNA

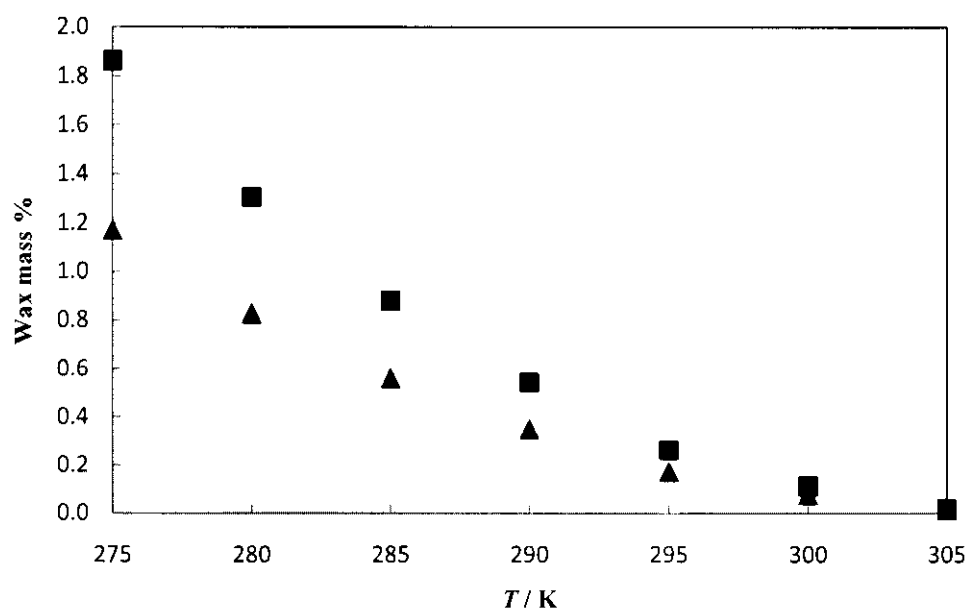


Figure 10: Wax amount against temperature for crude oil B. Symbols:
■, PNA; ▲, Without PNA

The model with the single solubility parameter correlation by Pedersen et al. [6] for paraffins and naphthenes, tends to give lower amount of wax in the crude oil A and B as shown in Figure 9 and Figure 10. The correlations for solid and liquid phase of C_7^+ are presented in Equation (22) and (23).

Meanwhile, the model that uses solubility parameter correlations for paraffins, naphthenes, and aromatic (PNA) gives higher amount of wax as the temperature decreases. The correlations are as in Equation (18)-(21).

From these results, the involvement of the naphthenic and aromatic components have definitely affected the amount of wax precipitated in the crude oil A and B. Components with similar molecular weight could have difference in the molecular structures either in naphthenic or aromatic compounds which can affect the solubility.

It is obvious that more detailed information about the hydrocarbon group type distribution is essential for the improvement of the model. For components with approximately the same molecular weight, the distinction must be made for paraffinic, naphthenic and aromatic compounds. In order to exploit detailed compositional information, accurate solubility data of different compounds have to be used in the model.

4.2.4 Effect of Solid-solid Transition

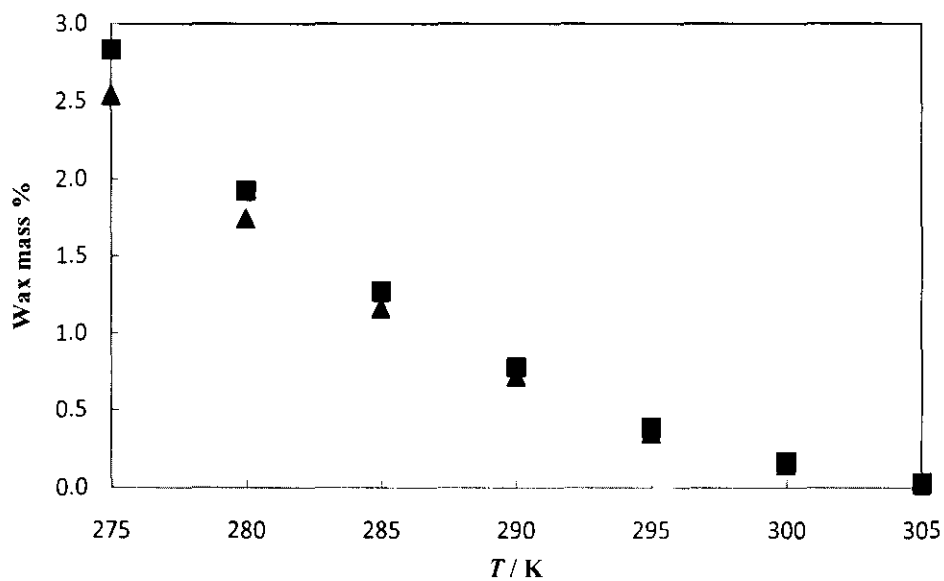


Figure 11: Wax mass percent against temperature for crude oil A with and without solid-solid transition. Symbols: ■, With solid-solid transition; ▲, Without solid-solid transition

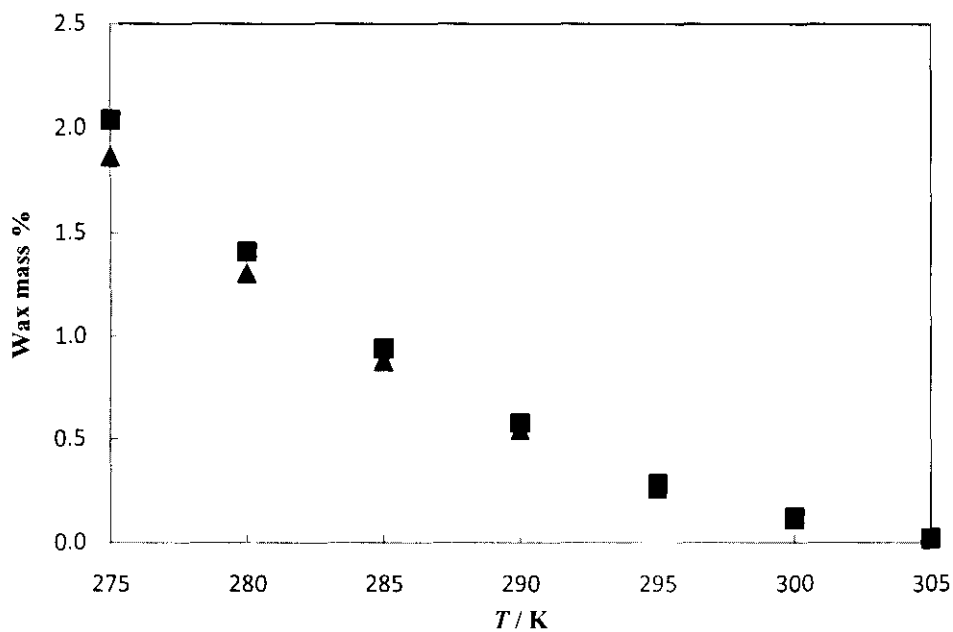


Figure 12: Wax mass percent against temperature for crude oil B with and without solid-solid transition. Symbols: ■, With solid-solid transition; ▲, Without solid-solid transition

The curves in Figure 11 and Figure 12 indicate that the solid-solid transition has effect to the amount of wax precipitated as temperature decreases. More solid wax will be formed if the solid-solid transition correlations are included in the thermodynamic model. The phase transition in the already formed wax is correlated by using the fusion temperature and fusion enthalpy as shown in Equation (32)-(35). The different parameters used in the fusion temperature and fusion enthalpy calculation will give significant effect to the wax precipitation. Thus, the calculations ought to take into consideration the phase transitions taking place in the already formed wax.

Due to phase transition, the wax will consist of two or more solid phases. The activity coefficients of solid phase are influenced by the phase composition as presented in Equation (11). The phase transition causes the compositions of each of the solid phases differ from that of the details of the total solid material.

4.2.5 Comparison of Model

By knowing the suitable parameters which include fusion temperature, fusion enthalpy and solubility parameters, a thermodynamic model can be developed to estimate the wax amount precipitated when the crude oil temperature drops. The results of this model are then being compared with the experiment results and the existing thermodynamic model.

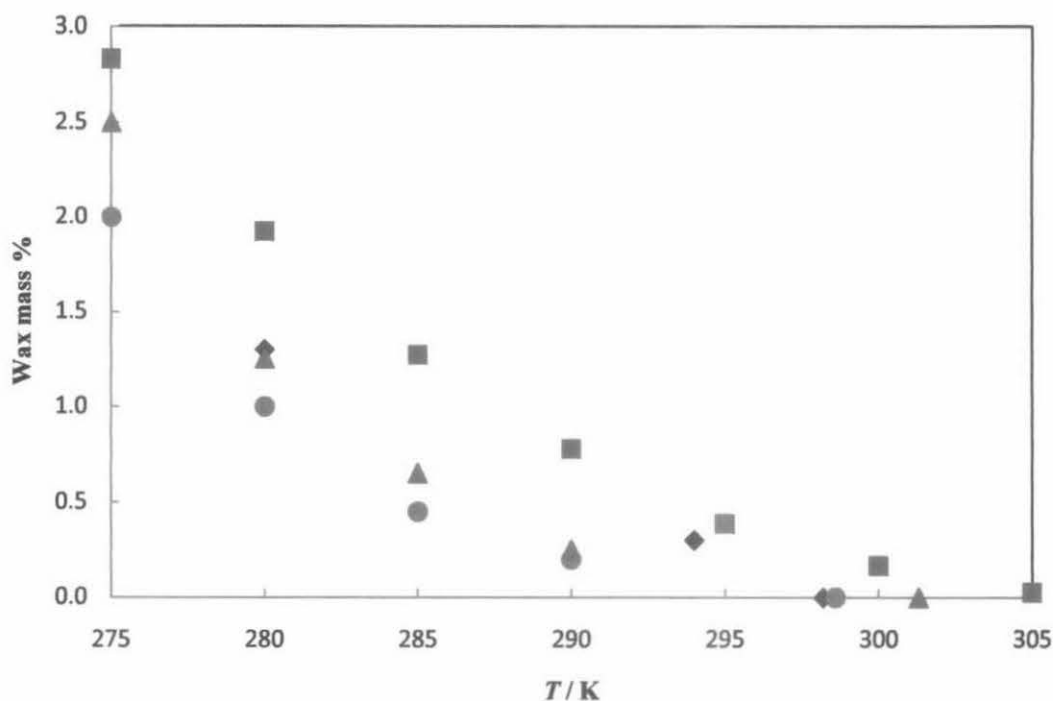


Figure 13: Comparison of model for crude oil A. Symbols: ■, This work; ▲, Chen's Model; ●, Leelavanichkul's Model; ◆, Experiment

Table 8: Experimental results and model predictions for crude oil A

Wax %	Experiment	Leelavanichkul		Chen		This work	
	T(K)	T(K)	Δ %	T(K)	Δ %	T(K)	Δ %
0.00	298.2	298.6	0.13	301.1	0.97	307.6	3.15
0.25	294.9	278.1	5.70	290.0	1.66	297.5	0.88
0.50	291.2	284.3	2.37	286.5	1.61	293.0	0.62
0.75	287.0	281.6	1.88	283.8	1.11	290.1	1.08
1.00	283.8	280.0	1.34	281.7	0.74	287.7	1.37
1.50	278.3	277.1	0.43	279.0	0.25	283.0	1.69

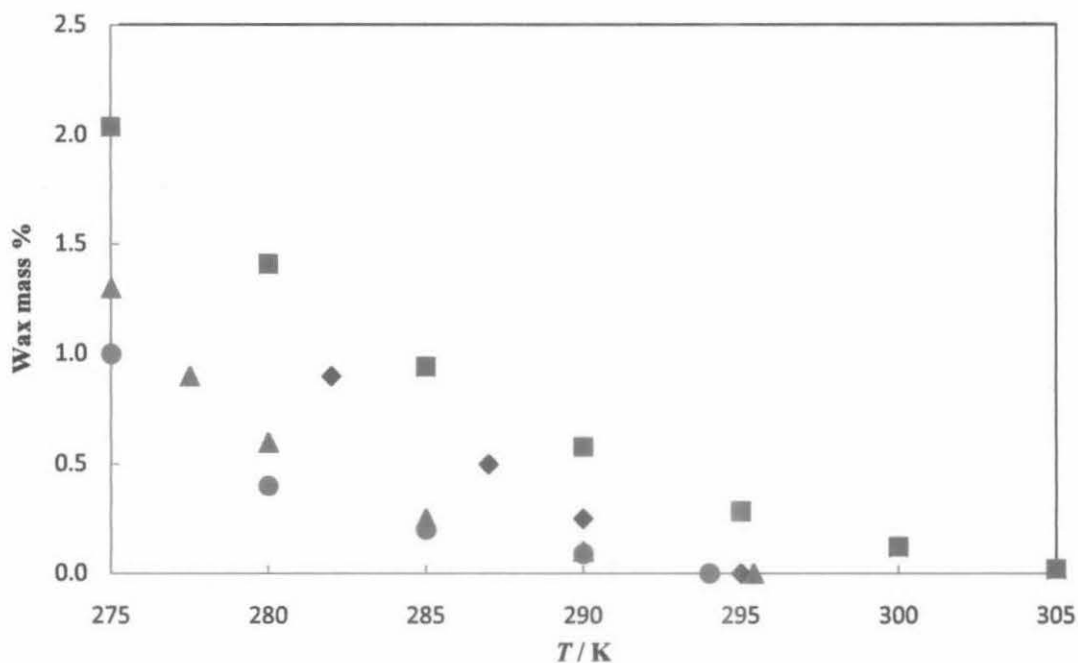


Figure 14: Comparison of model for crude oil B. Symbols: ■, This work; ▲, Chen's Model; ●, Leelavanichkul's Model; ◆, Experiment

Table 9: Experimental results and model predictions for crude oil B

Wax %	Experiment	Leelavanichkul		Chen		This work	
	T(K)	T(K)	Δ %	T(K)	Δ %	T(K)	Δ %
0.00	295.20	293.40	0.61	295.40	0.07	305.30	3.42
0.25	290.00	283.00	2.41	285.00	1.72	295.00	1.72
0.50	287.00	279.00	2.79	281.10	2.06	291.20	1.46
0.75	283.80	276.20	2.68	278.50	1.87	287.00	1.13
1.00	281.00	275.00	2.14	277.00	1.42	284.60	1.28

From Table 8, when compared to the existing models developed by Chen and Zhao [11] and Leelavanichkul et al. [12], the wax mass percent prediction of this work for crude oil A shows better estimates for the range of mass amount from 0.25 to 0.75 %. Meanwhile

for crude oil B better results are obtained for the range of wax amount from 0.25 to 1.00 % in Table 9. This is because the deviations of the temperatures from the experimental temperatures are smaller compared to the existing models. The results of this model indicate that the WATs are higher than the values predicted by the previous models. The model overestimates the WAT from experiment. This is due to the reason that the approaches of regular solid solution and ideal solid solution are used in this model. This model is based on solid solution theory which assumes the components in the solid phase are miscible in all proportions. However, the overestimation suggests that the solid solution is non-ideal. Higher temperature is better than lower temperature from the real temperature because early precautions can be taken to avoid the wax precipitation.

4.2.6 Potential Errors

There are some factors which would lead to significant errors in this modeling. The most obvious one will be the light fraction components. For this work, the first three carbon numbers (C1-C3) are being excluded due to mathematical error that it would raise. The model is started by taking C3 onwards. The main reason that directs the ignorance of the first three carbon numbers is because the molecular weight of these components in the crude oils is very small. Thus, when the molecular weight values are being inserted into Equation (26) for fusion temperature, negative value will be obtained. This later on will cause the thermodynamic equation to be undefined after integration where there is $\log T_i^f$. However, these three components are considered negligible as they possess very small fraction and molecular weight in the crude oils.

The non-n-alkane components of the crude oil samples A and B are also eliminated from the modeling process due to the reason that currently there is no complete correlation available from the literatures for calculation. There is only correlation obtainable for fusion temperature, T_i^f , but correlations for fusion enthalpy, H_i^f , solubility parameters, δ_i , and density are unavailable. The non-n-alkane components range from C26 to C50, so this would affect the accuracy of the model.

CHAPTER 5

CONCLUSION AND RECOMMENDATION

5.1 Conclusion

Specifying the suitable parameters of the proposed thermodynamic models can increase the accuracy of the Wax Appearance Temperature (WAT) prediction. The amount of wax precipitated will increase with the temperature drop. The objectives are achieved by considering different solubility parameters for components other than n-paraffins in crude oils such as naphthene and aromatic components. Together with that liquid-solid transition and solid-solid transition effects to the enthalpy change according to odd and even carbon numbers in wax formation also improved the prediction. The comparison of the thermodynamic model from this work with the existing models also shows encouraging results. When the model shows high accuracy to predict the WAT, appropriate mitigations can be carried out more efficiently to minimize the problems that would be caused by wax precipitation.

5.2 Recommendation

There are a number of thermodynamic models being proposed and each model possesses potencies and weaknesses. Recommendation will be to keep improving the parameters proposed to identify the suitable correlations. The solubility parameters and fusion enthalpies of the n-alkanes with different correlations according to the number of carbon atoms can improve the accuracy in the model. But further aspect that can be considered is to combine the thermodynamic model with flow model considering flow patterns, surface roughness and etcetera. The model also can be developed to calculate the heat transfer to the surrounding environment and the temperature profile in a pipeline. This is because the crude oil pipelines are installed on the seabed and in contact with sea water, so there is always heat transfer to the surrounding atmosphere.

Moreover, effects of pressure and pointing factor are also significant to the wax precipitation. Wax precipitation may occur at higher pressure conditions as the solidification temperature of carbon compounds may be increased. This would shift the wax phase boundary to higher temperature. Thus better focus is needed for the prediction of wax precipitation to improve the accuracy of the thermodynamic model.

REFERENCES

- [1] Boyun G., Shanhong S., Jacob C. and Ali G., 2005, *Offshore Pipelines*, Burlington, Gulf Professional Publishing
- [2] Abdul Aziz, Issham Ismail and Papathy S. 1999, *Managing Paraffin Wax Deposition in Oil Well*, Congress Paper, Universiti Teknologi Malaysia, Malaysia
- [3] Elsharkawy, A.M., Al-Sahhaf, T.A., Fahim, M.A., 2000, "Wax deposition from Middle East crudes", *Fuel* 79: 1047-1055
- [4] Ji, H.Y., Bahman, T., Ali, D., Adrian, C.T., 2004, "Wax phase equilibria: developing a thermodynamic model using a systematic approach", *Fluid Phase Equilibria*, 216(2), 201-217
- [5] Becker, J.R. 1997, *Crude Oil Waxes, Emulsions, and Asphaltenes*, South Sheridan, PennWell Publishing Company
- [6] Pedersen, K.S., Skovborg, P., Ronningsen, H.P., 1991, "Wax Precipitation from North Sea Crude Oils. 4. Thermodynamic Modeling", *Energy Fuels*, 5, 924-932
- [7] Hammami, A., Ratulowski, J., and Coutinho, A.P., 2003, "Cloud Points: Can We Measure or Model Them?" *Petroleum Science and Technology*
- [8] Burger, E.D., Perkins, T.K., and Striegler, J.H. 1981, "Studies of Wax Deposition in the Trans Alaska Pipeline", *J. of Petr. Tech.* 1075 – 1086
- [9] Won, K.W., 1986, "Thermodynamics for solid-liquid-vapor equilibria: wax phase formation from heavy hydrocarbon mixtures", *Fluid Phase Equilibria*, 30, 265-279

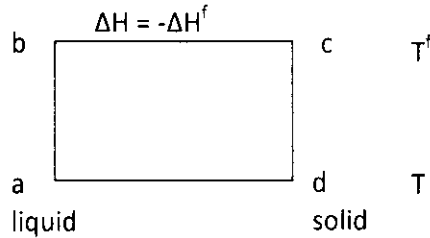
- [10] LiraGalena, C., Firoozabadi, A., Prausnitz, J.M., 1996, "Thermodynamics of wax precipitation in petroleum mixtures", *AIChEJ.*, 42, 239-248
- [11] Chen, W.H., Zhao, Z.C., 2006, "Thermodynamic Modeling of Wax Precipitation in Crude Oils", *Chinese Journal Chemical Engineering*, 14(5), 685-689
- [12] Leelavanichkul, P., Deo. M.D., Hanson, F.V., 2004, "Crude oil characterization and regular solution approach to thermodynamic modeling of solid precipitation at low pressure", *Petroleum Science and Technology*, 22(7/8), 973-990
- [13] Reza Dalirsefat, Farzaneh Feyzi, 2007, "A Thermodynamic Model for Wax Deposition Phenomena", *Fuel* 86, 1402-1408
- [14] J.M Smith, H. C. Van Ness, M. M. Abbott, 2001, *Introduction to Chemical Engineering Thermodynamics*, 6th ed., McGraw Hill Int.
- [15] Riazi, M.R., Al-Sahhaf, T.A., 1996, "Physical properties of heavy petroleum fractions and crude oils", *Fluid Phase Equilibria*, 117, 217-224
- [16] Broadhurst, M.GJ., 1962, "An analysis of the solid phase behavior of the normal paraffins", *Journal of Research of the National Bureau of Standards*, 66A, 241-249
- [17] Cutlip, M.B., Mordechai, S., 2008, *Problem Solving in Chemical and Biochemical Engineering with Polymath, Excel, and Matlab*, Upper Saddle River, NJ, Prentice Hall
- [18] Constantinides, A., 1999, *Numerical Method for Chemical Engineers with MATLAB Applications*, London, Prentice Hall
- [19] Musto, J.C., 2009, *Engineering Computations: An Introduction Using MATLAB and EXCEL*, Boston, McGraw-Hill Higher Education

APPENDICES

Appendix A

Derivation of Liquid-solid Transition Enthalpy:

The hypothetical process to calculate liquid-solid transition enthalpy at temperature, T lower than T^f can be represented as



The heat liberated is associated with the liquid-solid transition (a-d). To obtain this value, the process is started with a sub-cooled liquid to be heated from T to T^f . The enthalpy change is

$$\Delta H_{ab} = \int_T^{T^f} C_p^l dT$$

where C_p^l is the liquid phase heat capacity. At $T = T^f$ the liquid solidifies and this process is associated with the following enthalpy change:

$$\Delta H_{bc} = -\Delta H^f$$

Finally the solid is cooled from T^f to T . The enthalpy change is

$$\Delta H_{cd} = \int_{T^f}^T C_p^s dT$$

Where C_p^s is the molar heat capacity of the solid phase. The total enthalpy change is

$$\Delta H_{ad} = \Delta H_{ab} - \Delta H_{bc} - \Delta H_{cd}$$

Rewriting the equations will yield

$$\Delta H_{ad} = -\Delta H^f + \int_T^{T^f} (C_p^l - C_p^s) dT$$

Appendix B

Part of the model used in MATLAB software for Crude Oil A:

```
R=8.314;
T=280
%-----
%C1 to C6 Light

xis=[0.04563, 0.03342, 0.02486];
xil=1-xis;
mil=[58.1, 72.2, 82.0];

Tifl=374.5+0.02617.*mil-20172./mil;
Hifl=0.1426.*mil.*Tifl;
dil=0.815+0.06272E-4.*mil-13.06./mil;
Vil=mil./dil;

Al=(Hifl./(R*T)).*(1-(T./Tifl));
Bl=(1/(R*T)).*((1.2739.*mil.*Tifl-(1.9467E-3.*mil.*Tifl.^2)/2)-
(1.2739.*mil.*T-(1.9467E-3.*mil.*T^2)/2));
Cl=(1/R).*((1.2739.*mil.*log(Tifl)-1.9467E-3.*mil.*Tifl)-
(1.2739.*mil*log(T)-1.9467E-3.*mil*T));

Dl=Al-BL+Cl;

%fugacity ratio: fol/fos
folsl=exp(Dl);

phiLl=(xil.*Vil)/sum(xil.*Vil);
SPiLl=8.6-exp(2.219195-0.54907.*(mil.^0.3));
SPmLl=sum(phiLl.*SPiLl);
acLl=exp((Vil.*(SPmLl-SPiLl).^2)/(R*T));

phiSl=(xis.*Vil)/sum(xis.*Vil);
SPiSl=((Hifl./Vil)+(SPiLl).^2).^0.5;
SPmSl=sum(phiSl.*SPiSl);
acSl=exp((Vil.*(SPmSl-SPiSl).^2)/(R*T));

%-----

% Paraffin odd

xispo=[0.03343, 0.01659, 0.01171, 0.00748, 0.00510, 0.00433];
xilpo=1-xispo;
mipo=[128.3, 156.3, 184.4, 212.4, 240.5, 268.5];
Cpl=[9, 11, 13, 15, 17, 19];

Tifpo=374.5+0.02617.*mipo-20172./mipo;
Hifpo=0.5745.*mipo.*Tifpo;
```

```

dipo=0.815+0.06272E-4.*mipo-13.06./mipo;
Vipo=mipo./dipo;

Apo=(Hifpo./(R*T)).*(1-(T./Tifpo));
Bpo=(1/(R*T)).*((1.2739.*mipo.*Tifpo-(1.9467E-3.*mipo.*Tifpo.^2)/2)-
(1.2739.*mipo.*T-(1.9467E-3.*mipo.*T^2)/2));
Cpo=(1/R).*((1.2739.*mipo.*log(Tifpo)-1.9467E-3.*mipo.*Tifpo)-
(1.2739.*mipo*log(T)-1.9467E-3.*mipo*T));

Dpo=Apo-Bpo+Cpo;

%fugacity ratio: fol/fos
folspo=exp(Dpo);

phiLpo=(xilpo.*Vipo)/sum(xilpo.*Vipo);
SPiLpo=7.41+0.5914.*(log(Cp1)-log(7));
SPmLpo=sum(phiLpo.*SPiLpo);
acLpo=exp((Vipo.*(SPmLpo-SPiLpo).^2)/(R*T));

phiSpo=(xispo.*Vipo)/sum(xispo.*Vipo);
SPiSpo=8.50+5.763.*(log(Cp1)-log(7));
SPmSpo=sum(phiSpo.*SPiSpo);
acSpo=exp((Vipo.*(SPmSpo-SPiSpo).^2)/(R*T));

% Paraffin even

xispe=[0.04237, 0.02438, 0.01174, 0.00916, 0.00591, 0.00451, 0.00309];
xilpe=1-xispe;
mipe=[114.2, 142.3, 170.3, 198.4, 226.4, 254.5, 282.5];
Cp2=[8, 10, 12, 14, 16, 18, 20];

Tifpe=374.5+0.02617.*mipe-20172./mipe;
Hifpe=0.8064.*mipe.*Tifpe;
dipe=0.815+0.06272E-4.*mipe-13.06./mipe;
Vipe=mipe./dipe;

Ape=(Hifpe./(R*T)).*(1-(T./Tifpe));
Bpe=(1/(R*T)).*((1.2739.*mipe.*Tifpe-(1.9467E-3.*mipe.*Tifpe.^2)/2)-
(1.2739.*mipe.*T-(1.9467E-3.*mipe.*T^2)/2));
Cpe=(1/R).*((1.2739.*mipe.*log(Tifpe)-1.9467E-3.*mipe.*Tifpe)-
(1.2739.*mipe*log(T)-1.9467E-3.*mipe*T));

Dpe=Ape-Bpe+Cpe;

%fugacity ratio: fol/fos
folspe=exp(Dpe);

phiLpe=(xilpe.*Vipe)/sum(xilpe.*Vipe);
SPiLpe=7.41+0.5914.*(log(Cp2)-log(7));
SPmLpe=sum(phiLpe.*SPiLpe);
acLpe=exp((Vipe.*(SPmLpe-SPiLpe).^2)/(R*T));

phiSpe=(xispe.*Vipe)/sum(xispe.*Vipe);

```

```

SPiSpe=8.50+5.763.*(log(Cp2)-log(7));
SPmSpe=sum(phiSpe.*SPiSpe);
acSpe=exp((Vipe.*(SPmSpe-SPiSpe).^2)/(R*T));

%-----

% C7-C25 Napthenic

xisn=[0.01812, 0.01747, 0.01742, 0.01512, 0.01281, 0.01189, 0.01226,
0.01097, 0.00967, 0.00810, 0.00724, 0.00664, 0.00509, 0.00446, 0.00363,
0.00310, 0.00250, 0.00226, 0.00203];
xiln=1-xisn;
min=[96.8, 110.6, 124.4, 138.2, 152.1, 165.9, 179.7, 193.5, 207.4,
221.2, 235.0, 248.8, 262.7, 276.5, 290.3, 304.1, 318.0, 331.8, 345.6];
Cp4=[7, 8, 9, 10, 11, 12, 13, 14, 15, 16, 17, 18, 19, 20, 21, 22, 23,
24, 25];

Tifn=374.5+0.02617.*min-20172./min;
Hifn=0.1426.*min.*Tifn;
din=0.865+0.06272E-4.*min-13.06./min;
Vin=min./din;

An=(Hifn./(R*T)).*(1-(T./Tifn));
Bn=(1/(R*T)).*((1.2739.*min.*Tifn-(1.9467E-3.*min.*Tifn.^2)/2)-
(1.2739.*min.*T-(1.9467E-3.*min.*T.^2)/2));
Cn=(1/R).*((1.2739.*min.*log(Tifn)-1.9467E-3.*min.*Tifn)-
(1.2739.*min*log(T)-1.9467E-3.*min*T));

Dn=An-Bn+Cn;

%fugacity ratio: fol/fos
folsn=exp(Dn);

phiLn=(xiln.*Vin)/sum(xiln.*Vin);
SPiLn=7.41+0.5914.*(log(Cp4)-log(7));
SPmLn=sum(phiLn.*SPiLn);
acLn=exp((Vin.*(SPmLn-SPiLn).^2)/(R*T));

phiSn=(xisn.*Vin)/sum(xisn.*Vin);
SPiSn=8.50+5.763.*(log(Cp4)-log(7));
SPmSn=sum(phiSn.*SPiSn);
acSn=exp((Vin.*(SPmSn-SPiSn).^2)/(R*T));

%-----

```

```
% C7-C50 Aromatic
```

```
xisa=[0.01609, 0.01766, 0.01883, 0.01711, 0.01523, 0.01555, 0.01673,  
0.01678, 0.01665, 0.01466, 0.01349, 0.01338, 0.01305, 0.01219, 0.01100,  
0.01046, 0.00941, 0.00853, 0.00766, 0.00445, 0.00352, 0.00352, 0.00337,  
0.003, 0.00293, 0.00256, 0.00246, 0.00221, 0.00202, 0.00193, 0.00183,  
0.0017, 0.00162, 0.00148, 0.00138, 0.0014, 0.00121, 0.00117, 0.0011,  
0.00109, 0.00095, 0.00093, 0.00081, 0.00079];
```

```
xila=1-xisa;
```

```
mia=[91.1, 104.1, 117.2, 130.2, 143.2, 156.2, 169.2, 182.3, 195.3,  
208.3, 221.3, 234.3, 247.3, 260.4, 273.4, 286.4, 299.4, 312.4, 325.5,  
338.5, 351.5, 364.5, 377.5, 390.5, 403.6, 416.6, 429.6, 442.6, 455.6,  
468.6, 481.7, 494.7, 507.7, 520.7, 533.7, 546.8, 559.8, 572.8, 585.8,  
598.8, 611.8, 624.9, 637.9, 650.9];
```

```
Tifa=374.5+0.02617.*mia-20172./mia;
```

```
Hifa=0.1426.*mia.*Tifa;
```

```
dia=-0.03.*log(mia)+1.02;
```

```
Via=mia./dia;
```

```
Aa=(Hifa./(R*T)).*(1-(T./Tifa));
```

```
Ba=(1/(R*T)).*((1.2739.*mia.*Tifa-(1.9467E-3.*mia.*Tifa.^2)/2)-  
(1.2739.*mia.*T-(1.9467E-3.*mia.*T^2)/2));
```

```
Ca=(1/R).*((1.2739.*mia.*log(Tifa)-1.9467E-3.*mia.*Tifa)-  
(1.2739.*mia*log(T)-1.9467E-3.*mia*T));
```

```
Da=Aa-Ba+Ca;
```

```
%fugacity ratio: fol/fos
```

```
folsa=exp(Da);
```

```
phiLa=(xila.*Via)/sum(xila.*Via);
```

```
SPiLa=8.8-exp(2.219195-0.54907.*(mia.^0.3));
```

```
SPmLa=sum(phiLa.*SPiLa);
```

```
acLa=exp((Via.*(SPmLa-SPiLa).^2)/(R*T));
```

```
phiSa=(xisa.*Via)/sum(xisa.*Via);
```

```
SPiSa=((Hifa./Via)+(SPiLa).^2).^0.5;
```

```
SPmSa=sum(phiSa.*SPiSa);
```

```
acSa=exp((Via.*(SPmSa-SPiSa).^2)/(R*T));
```

```
%-----
```

```
%acL: activity coefficient for liquid
```

```
%acS: activity coefficient for solid
```

```
%S: solid mole fraction
```

```
S=0.5;
```

```
%kisl=xiS/xiL
```

```
kisl1=(acL1/acS1).*fols1;
```

```
kislpo=(acLpo/acSpo).*folspo;
```

```
kislpe=(acLpe/acSpe).*folspe;
```

```
kislpx=(acLpx/acSpx).*folspx;
```

```
kisln=(acLn/acSn)*folsn;  
kisla=(acLa/acSa)*folsa;
```

```
waxmass=sum(sum(mil.*xiSl.*S)+sum(mipo.*xiSpo.*S)+sum(mipe.*xiSpe.*S)+  
sum(mipx.*xiSpx.*S)+sum(min.*xiSn.*S)+sum(mia.*xiSa.*S))/sum(sum(mil.*xi  
s)+sum(mipo.*xispo)+sum(mipe.*xispe)+sum(mipx.*xispx)+sum(min.*xisn)+su  
m(mia.*xisa))
```